Kanikode Abdul Latheef Abdul Rahman, Deepti Hariharan
Group P3

Advanced Lab Course: Optical Frequency Doubling – A245

5 & 6 August 2019
Tutor: Benjamin Rauf
Universität Bonn

Contents

1. Theory

1.1. Diode Laser

A typical laser diode system has a sandwich of two semiconductor of P type and N type in a forward bias configuration, a resonator and a collimator. When current is passed through this diode, electron-hole pairs are created at the junction. Due to the energy difference between the electron and hole, combination of this pair emit photons which is of fixed energy. This energy difference corresponds to the band gap of the material used. Using a resonator with partial reflecting mirrors the light is amplified and stimulated emission is achieved. The out-coming light of this resonator is collimated to get what we call LASER light.

1.2. Gaussian Beam

A Gaussian beam is the solution of a product of a rapidly varying plane wave E(x,y,z) and a slowly varying envelope U(x,y,z) of the Helmholtz equation:

$$E(x, y, z) = U(x, y, z)\ exp(-ikz)$$

The Gaussian beam describes the linear phase fronts in the beam focus and also the radial behavior in the far field. A sketch of a Gaussian beam is shown in fig. 1.1.

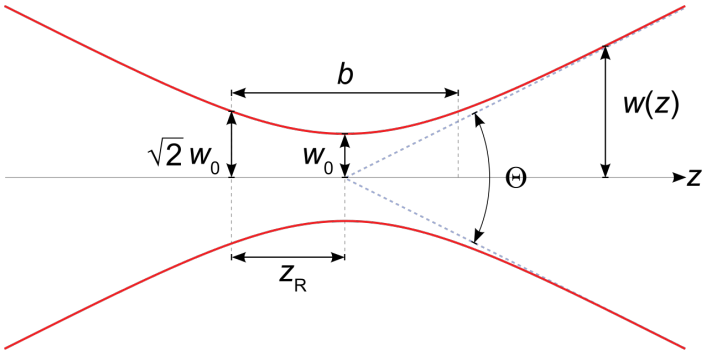

Figure 1.1.: A Gaussian beam propagating along z-axis (source: Wikipedia, author: DrBob)

1.2.1. Beam waist

For a beam of diameter d and wavelength of light λ, the beam waist is given as:

$$w_0 = \frac{\lambda f}{\pi d}$$

where f is the focal length of the lens used to focus the beam.

1.2.2. Rayleigh length & Confocal Parameter

For a medium of refractive index n, the Rayleigh length is given by:

$$z_R = \frac{\pi n w_0^2}{\lambda}$$

and the confocal parameter, b is the distance between the points $+z_R$ and $-z_R$:

$$b = 2z_R = \frac{2\pi n w_0^2}{\lambda}$$

1.2.3. Beam radius

$$w(z) = \sqrt{1+\left(\frac{z}{z_R}\right)^2}$$

where z is the distance along the beam.

1.2.4. Radius of curvature

$$R(z) = z\left(1+\left(\frac{z_R}{z}\right)^2\right)$$

.

1.2.5. Boyd-Kleinmann condition

The intensity of the harmonic wave is maximum if it fulfills the Boyd-Kleinmann condition:

$$\frac{L}{b} = 2.84$$

where L is the crystal length.

1.3. Birefringence

Birefringence is optical property seen in certain materials depending on the crystal structure. The refractive index of these material are anisotropic in nature along different axes and hence depending on the direction of propagation of light and the polarization along that direction, these axes are called ordinary and extraordinary axis. Light propagating parallel to the optical axis is called the ordinary beam and 'sees' refractive index n_o and light propagating perpendicular to the optical axis is called the extraordinary beam and it 'sees' refractive index n_e. The extraordinary axis is called the optical axis. Uniaxial crystals have two refractive indices, i.e., refractive index of one axis is different from the other two. On the other hand, in biaxial crystals, the index is different along all three axis. The values of n_0 and n_e determine if the birefringence is positive ($n_0 > n_e$) or negative ($n_0 < n_e$).
The extraordinary and ordinary beams emerge with an angle θ. The refractive index of the extraordinary beam is given by:

$$\frac{1}{n_e(\theta)} = \frac{cos^2\theta}{n_o^2} + \frac{sin^2\theta}{n_e^2}$$

1.4. Second Harmonic Generation

In a non-linear dielectric media the polarization due to the applied electric field **E** is given by:

$$\mathbf{P} = \epsilon_0 \left[\chi^{(1)}\mathbf{E} + \chi^{(2)}\mathbf{E}^2 + \chi^{(3)}\mathbf{E}^3 \dots \right]$$

where ϵ_0 is the permittivity of free space.

$$P = P_{linear} + P_{non-linear}$$

Now consider two plane electric field $E_1(\omega_1)$ and $E_2(\omega_2)$ propagating along k_1 and k_2 through a non-linear (anisotropic) medium. The interaction of these two fundamental waves $E_1(\omega_1)$ and $E_2(\omega_2)$ induces polarization in the dielectric medium. The non-linear term is of the interest as this non-linear polarization acts as source to generating signals $E_3(\omega_3)$ called the higher order harmonic waves with frequencies the sum and difference of the fundamental frequencies ω_1 and ω_2.
In a similar fashion when we use only one fundamental wave $E(\omega)$ with a single frequency ω (along the direction of propagation k), the harmonic wave generated has sum frequency as twice the fundamental frequency and difference zero. Since the generated harmonic wave is has twice the frequency of the fundamental wave, we call it second harmonic generation (SHG). Since the magnitude of propagation vector of fundamental wave k_ω and second harmonic wave $k_{2\omega}$ are different ($\Delta k = 2k_\omega - k_{2\omega}$), the two waves are not in phase with each other and hence the intensity of the generated SHW oscillates with distance along its axis of propagation with a period $l_c = \pi/\Delta k$, called the coherence length. To make the second harmonic (SH) wave more efficient we require phase matching.

1.5. Phase Matching

The intensity of the second harmonic wave oscillates along the direction of propagation. It can be shown to be:

$$I_{SH} = \Gamma^2 l^2 I_{FUN}^2 \frac{sin^2(\Delta kl/2)}{(\Delta kl/2)^2}$$

where Γ depends on the properties of the material and l is the length of the crystal. The magnitude of the phase mismatch tells us how the intensity of the harmonic wave oscillates between the fundamental and harmonic wave when propagating in a crystal as shown in fig. 1.2a, and fig. 1.2b gives us the clear picture as to what range (magnitude of $\Delta kl/2$ is less than π) the SH intensity is more efficient. For perfect phase matching, the mismatch should be zero ($\Delta k = 0$).

$$\Delta k = k_{2\omega} - k_w = \frac{2\omega}{c}(n_{2\omega} - n_\omega) = 0$$

$$\therefore, n_{2\omega} = n_\omega$$

Hence, by matching the refractive index of the two waves an efficient SH can be generated. This kind of index matching is also known as Type I phase matching. Type II phase matching condition requires that the propagation of $P_{non-linear}$ through the crystal must have the same phase velocity as the second harmonic wave.

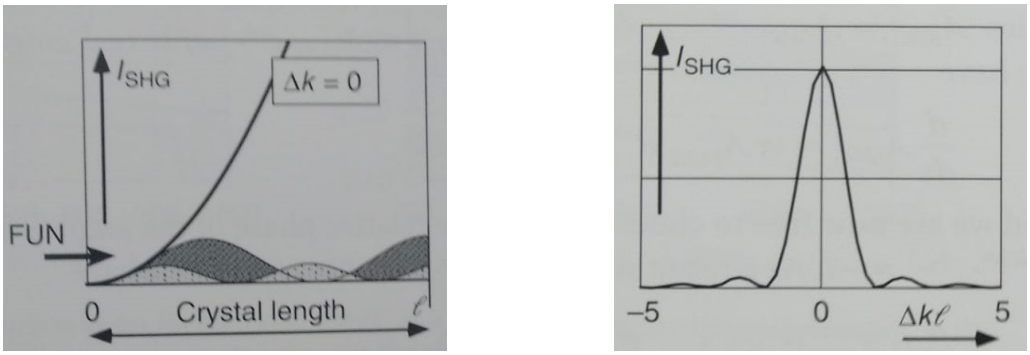

(a) **(b)**

Figure 1.2.: Variation of the second harmonic wave with respect to the crystal length(a) and phase mismatch(b) (source [4])

1.6. Diffraction Grating

The grating used in this experiment is the reflective type. It consists of many slits each of width d as shown in fig. 1.3. A monochromatic light of wavelength λ is incident on the grating is reflected off the slits and each reflected wave interferes with one another to form a diffraction pattern. The grating equation is:

$$m\lambda = d(sin\ \theta_i - sin\ \theta_m)$$

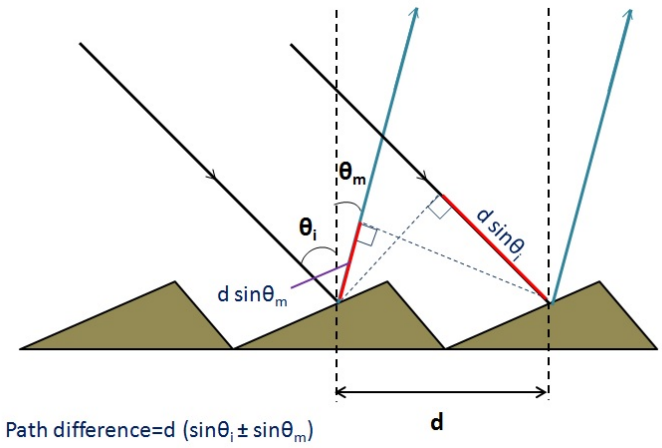

Figure 1.3.: Reflective diffraction grating (source: Wikipedia; author: Vigneshdm1990)

1.7. Michelson Interferometer

A Michelson consists of a beam splitter which splits the incoming light into two. One beam is reflected onto itself by a fixed mirror and the other by a movable end mirror as shown in fig. 1.4. Both the reflected beams are then recombined and detected. If the setup is arranged properly, it is possible to

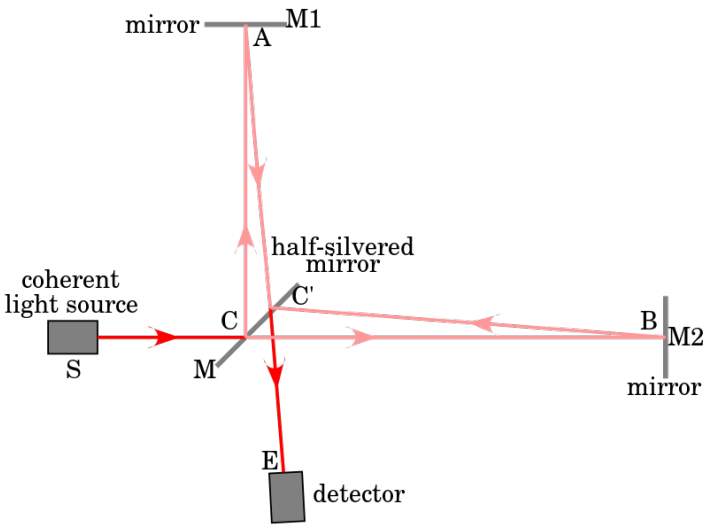

Figure 1.4.: Scematic diagram of a Michelson interferometer (source: Wikipedia; author:Krishnavedala)

see interference fringes of different orders in the whole length of the movable end-mirror. The detected beam is read on an oscilloscope in the form of Lissajous figures.

2. Diode Laser and Power Measurements

First, we studied the diode laser. We used a commercial, grating-stabilized (Littrow) external cavity diode laser system. A shutter is placed after the laser which is connected to the safety interlock system to control the beam. An anamorphic prism pair converts the elliptical beam to a more circular one.

2.1. Laser Output Power vs. Injection Current

We measure the laser output power while varying the injection current to the laser from 0 - 280 mW. The readings are given in table A.1. The plot was fitted with a linear function of the form:

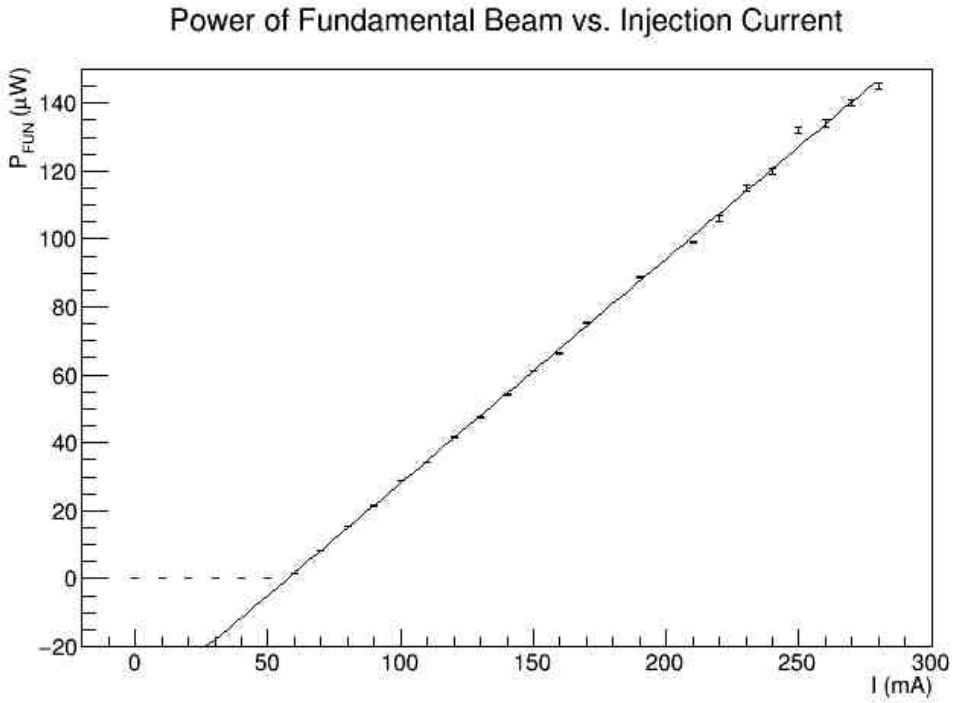

Figure 2.1.: Power of fundamental beam vs the injection current

$$P = mI + c$$

as shown in fig. 2.1 using ROOT. The threshold current obtained from the graph is:

$$I_{th} = 57.30\ mA$$

The differential slope efficiency was found from the plot to be:

$$\frac{\partial P}{\partial I} = m = (0.66 \pm 0.005)\ \mu W/mA$$

Using this, the differential quantum efficiency was calculated:

$$\eta = \frac{N_\gamma}{N_e} = \frac{me\lambda}{hc} = (49.9 \pm 0.4)\ \%$$

2.2. Calibration of Variable Attenuator

In order to keep the diode current constant while varying the laser power, we have to calibrate the attenuator. To do so, a half-wave plate is used in combination with a polarizer. The λ/2 plate kept perpendicular to the beam rotates the linear polarization and the polarizer transmits only one component of the beam.
We change the rotation angle of the λ/2 plate an measure the power of the beam in the power meter. The readings are tabulated in table A.2. The intensity of the light through the polarizer follows Malus' law. We expect a squared cosine dependence on the angle of rotation. The data was fitted with a function of the form:

$$P(\theta) = P_1\ cos^2(\ a(\theta - b)\ ) + P_0$$

The plot is shown in fig. 2.2. The fit parameters as given by ROOT are:

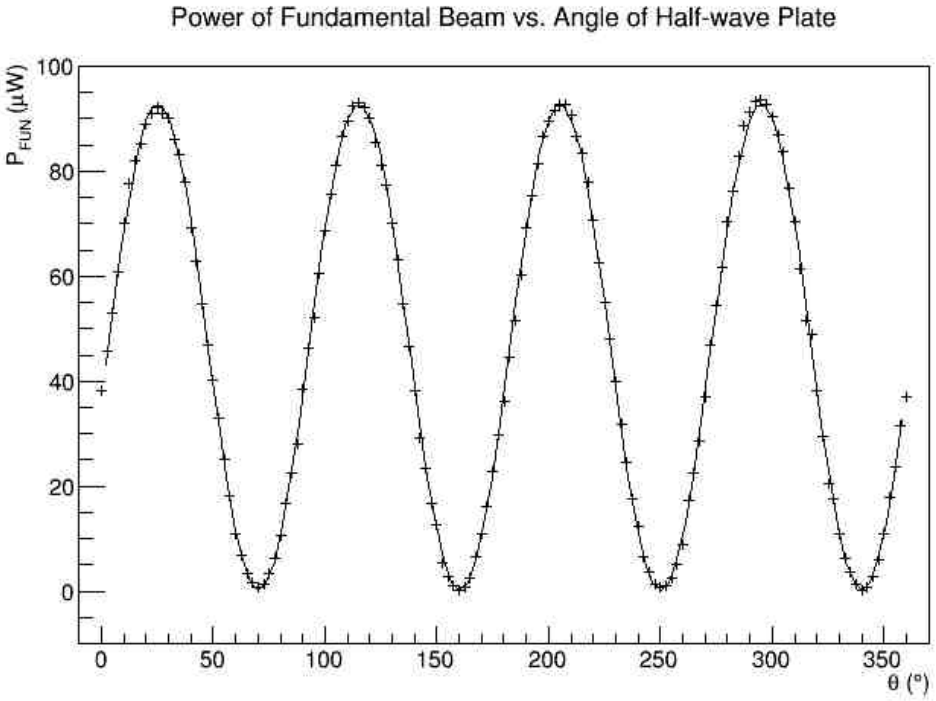

Figure 2.2.: Power of fundamental beam vs. angle of λ/2 plate

$$P_0 = (0.128 \pm 0.097)\ \mu W$$

$$P_1 = (92.66 \pm 0.16)\ \mu W$$

$$a = 2.001 \pm 0.0005$$

$$b = 25.32 \pm 0.043$$

P_0 is the minimum power coming out of the polarizer, a gives the variation of phase and b gives the phase change. The extinction ratio is:

$$e = \frac{P_1 + P_0}{P_0} = 726.09 \pm 551.2$$

3. Focusing the Laser Beam Into the Crystal and Optimizing the Harmonic Power

A f = 60 mm plano-convex lens is set perpendicular to the beam with the curved side facing the beam to focus the light into the birefringent crystal. The frequency-doubled light was collimated using an achromatic lens. A 3mm BG40 glass filter and a stray-light shielding tube was placed after the crystal to filter the infrared light for fine optimization of the harmonic wave. The setup is shown in fig. 3.1.

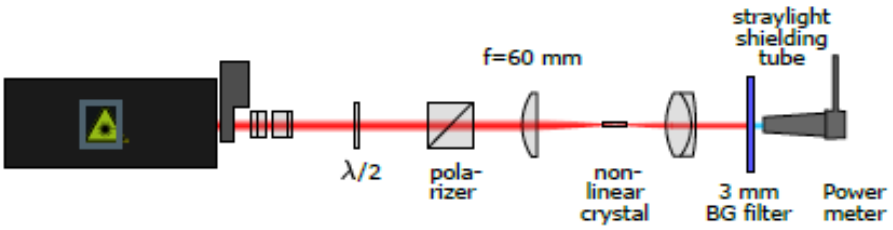

Figure 3.1.: Setup for measuring harmonic power [1]

3.1. Optimization of Second Harmonic Power

The temperature of the crystal was slowly increased in steps of 0.5°C up to 36°C which is the optimum temperature for second-harmonic generation for $KbNO_3$ crystal.

Analysis and Interpretation
The collimated beam has a diameter d = (3.5 ± 0.5) mm before the lens of focal length f = 60 mm. The approximate value of the refractive index of the crystal is n = 2.2 and the length of the crystal is L = (5.0 ± 0.5) mm. The wavelength of the light λ= 987 nm.

The beam waist is given by:

$$w_0 = 2\frac{\lambda f}{\pi d} = (10.78 \pm 1.54)\,\mu m$$

The Rayleigh length is calculated as:

$$z_0 = \frac{\pi n w_0^2}{\lambda} = (8.14 \pm 2.32) \times 10^{-4}\,m$$

The confocal parameter is then:

$$b = 2z_0 = (16.28 \pm 4.64) \times 10^{-4}\,m$$

The length to confocal parameter ratio is $\frac{L}{b} = (3.07 \pm 0.93)$. This value satisfies the Boyd-Kleinman condition within the error range.
Using the ideal ratio, we calculate the optimum focal length:

$$\frac{L}{b} = \frac{L}{\frac{2n\pi w_0^2}{\lambda}} = 2.84$$

$$\implies \frac{2\pi n(\frac{2\lambda f}{\pi d})^2}{\lambda} = \frac{L}{2.84}$$

$$\therefore f = \sqrt{\frac{L\pi d^2}{8n\lambda \cdot 2.84}}$$

The error in f is calculated as:

$$\Delta f = \sqrt{\frac{\pi}{8n\lambda \cdot 2.84}} \sqrt{\frac{1}{4}\Delta L^2 \cdot d^2 + \Delta d^2 \cdot L}$$

Hence, the optimum focal length using the Boyd-Kleinman condition is $f = (62.5 \pm 8.9)\ mm$

4. Properties of Second-Harmonic Generation

4.1. Harmonic Power vs. Crystal Temperature

The setup was not changed any further. The temperature of the crystal was decreased to 27°C and then increased to 40°C in steps of 0.2°. The power of the harmonic wave was measured with the power meter. The readings are tabulated in table A.3.
The data was fitted with a *sinc* function of the form:

$$P_{SH} = P_1 \left(\frac{sin(\ a(T-t)\ )}{a(T-t_r)} \right)^2 + P_0$$

The plot is shown in fig. 4.1. The parameters obtained from the fit are:

$$P_0 = (0.23 \pm 0.03)\ \mu W$$

$$P_1 = (13.32 \pm 0.12)\ \mu W$$

$$a = (2.15 \pm 0.02)\ /^\circ C$$

$$t_r = (36.53 \pm 0.006)\ /^\circ C$$

P_0 gives the offset in the power of the second harmonic, P_1 is the maximum power, a is the variation in phase and t_r is the resonance temperature at which the maxima occurs.
The see the minima and second maxima more clearly, we plotted the logarithm of the second harmonic power vs. the temperature of the crystal, as shown in fig. 4.2.
The curve could be asymmetric due to a few factors such as refractive indices of the crystal and lenses being non-linear, temperature sensitivity of the crystal which may change it's form temporarily.

4.2. Harmonic Power vs. Fundamental Wave Power

The temperature of the crystal was set to th optimum temperature of 36.4°C. The power of the harmonic wave was then measured relative to the angle of the λ/2 plate. Rotation of the λ/2 plate leads to the polarization of both the harmonic and fundamental waves as the polarizing beam splitter cube is still in the path of the beam. The data is presented in table A.2.
The relation between the power of harmonic and fundamental waves is expected to be:

$$P_{SH} = c \cdot P_{FUN}^2$$

c contains all the constant parameters of the crystal. The plot is shown in fig. 4.3. As we can see, there are no significant deviations and the values are as expected. This means that the phases of the harmonic and fundamental waves are not significantly different and phase matching is possibly achieved. The frequency doubling efficiency is:

$$\eta = \frac{P_{SH}}{P_{FUN}^2} = c$$

The value of c as obtained from the fit is:

$$c = \eta = (1.57 \pm 0.000008) \cdot 10^{-3} \mu W^{-1}$$

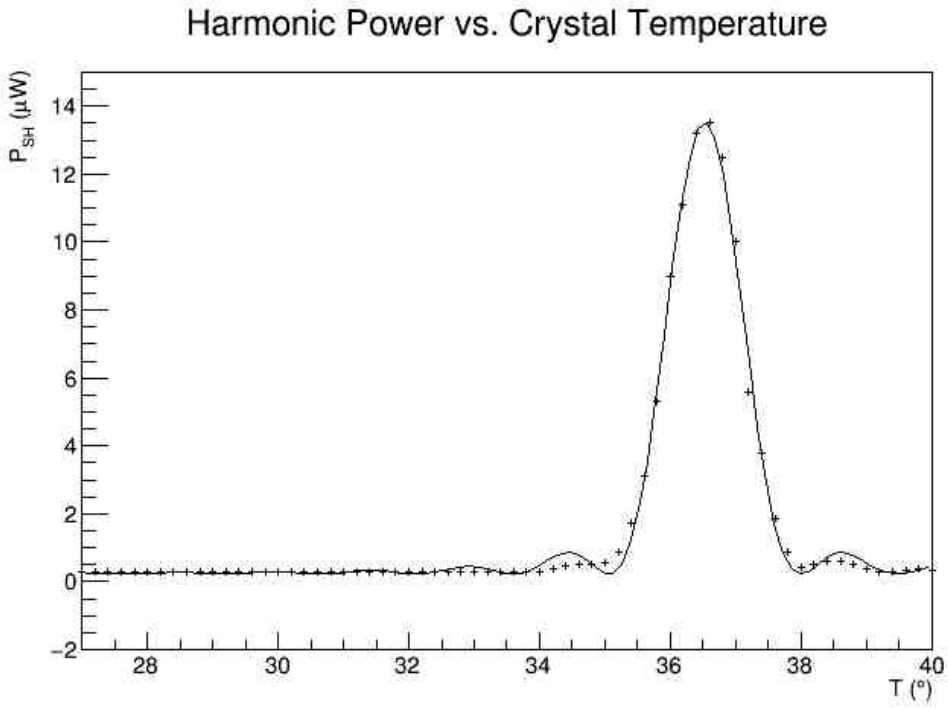

Figure 4.1.: Power of second harmonic beam vs. crystal temperature

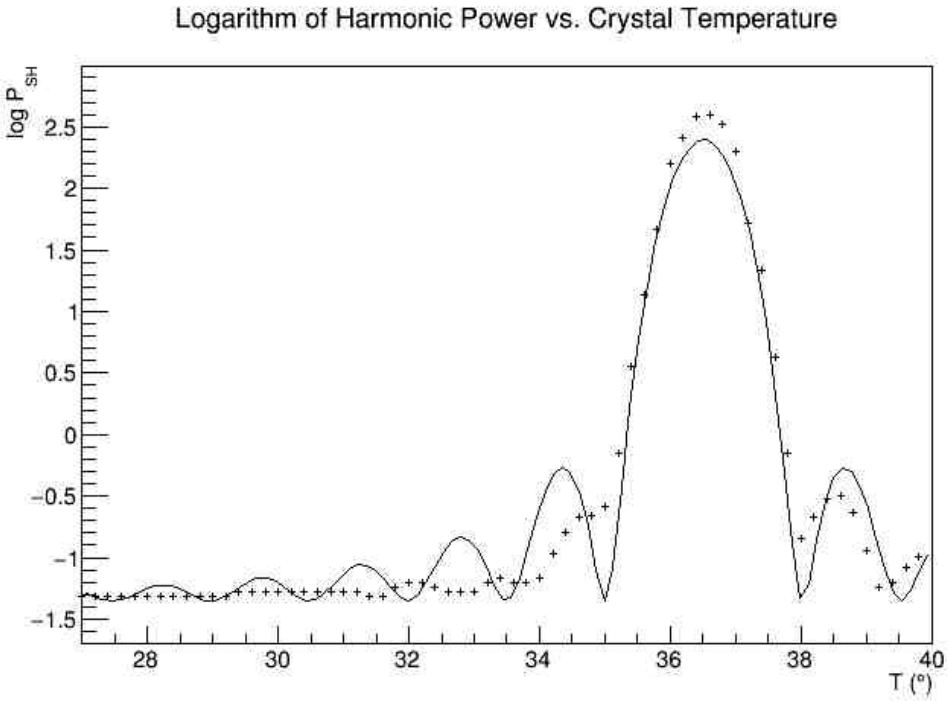

Figure 4.2.: Logarithm of power of second harmonic beam vs. crystal temperature - the minima and second maxima is seen more clearly in this graph

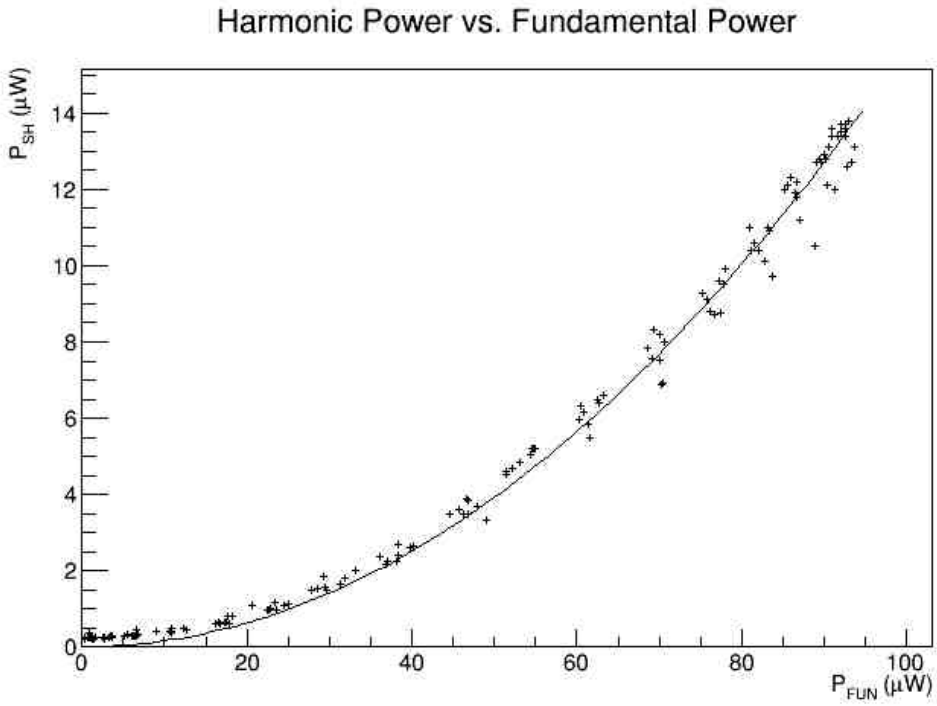

Figure 4.3.: Power of second harmonic vs. power of fundamental beam

4.3. Harmonic Power vs. Polarization of Fundamental Wave

The polarizing beam splitter cube was then removed and the linear polarization of the fundamental wave was rotated by varying the angle of the λ/2 plate. The data can be found in table A.4.
Depending on the phase matching achieved, different results were expected; for type I phase matching, we expect a dependence of the form:

$$P_{SH} \propto cos^4\theta$$

and for type II phase matching, we expect:

$$P_{SH} \propto cos^2\theta\ sin^2\theta$$

The data was fitted with boh the types. The fit for type I was the closest fit as shown in fig. 4.4. The fit function was:

$$P = c \cdot cos^4\left(\frac{\theta - a}{b}\right)$$

The fit parameters obtained are:

$$a = (-24.0013 \pm 0.09)^\circ$$

$$b = (0.499 \pm 0.0003)^\circ$$

$$c = (12.04pm0.03)\ \mu W$$

a gives the phase difference and since it is well less than 90°, we can conclude that it is a good $cos^4\theta$ fit. Therefore, type I phase matching was achieved.

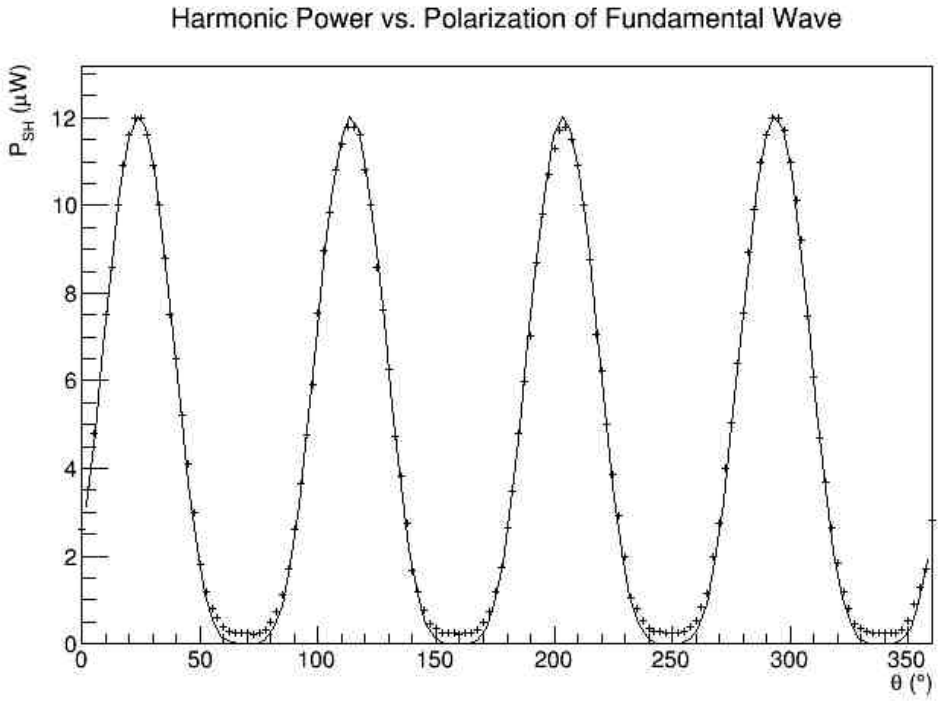

Figure 4.4.: Power of harmonic beam vs. polarization of fundamental beam

5. Comparison of Wavelengths of Fundamental and Harmonic Waves

5.1. Diffraction Grating

We used a 600 lines/mm grating to roughly compare the wavelengths of the fundamental and second harmonic waves. The harmonic beam is expected to have half the wavelength of the fundamental beam. The beam was collimated using a f = 60mm lens placed perpendicular to he beam and at the center. The grating was then placed in the path of the beam and different orders of the fundamental and harmonic beams were observed. A rough sketch of the setup is shown in fig. 5.1. Comparison of the n^{th} order of the fundamental and the $2n^{th}$ order of the harmonic informs us about the ratio of the wavelengths of the two beams.
The various lengths were measured to be:

$$L = (89 \pm 1)\ cm$$

$$w_1 = (30 \pm 0.4)\ cm$$

$$w_2 = (35 \pm 0.4)\ cm$$

The angles are calculated as:

$$\theta_1 = tan^{-1}\left(\frac{w_1 + w_2}{L}\right)$$

$$\theta_2 = tan^{-1}\left(\frac{w_1}{L}\right)$$

The errors in the angles are:

$$\Delta\theta_1 = \left(\frac{1}{1+\left(\frac{w_1+w_2}{L}\right)^2}\frac{1}{L}\sqrt{\Delta w_1^2 + \Delta w_2^2 + \frac{\Delta L^2 (w_1+w_2)^2}{L^2}}\right) \times \frac{180}{\pi} \quad degrees$$

$$\Delta\theta_2 = \left(\frac{1}{1+\left(\frac{w_1}{L}\right)^2}\frac{1}{L}\sqrt{\Delta w_1^2 + \frac{\Delta L^2 w_1^2}{L^2}}\right) \times \frac{180}{\pi} \quad degrees$$

The value of the angles are then:

$$\theta_1 = (36.142 \pm 0.39)^\circ$$

$$\theta_2 = (18.628 \pm 0.30)^\circ$$

The wavelengths are calculated using the angles by:

$$\lambda = \frac{d}{n}(sin\ \alpha - sin\ (\alpha - \theta)\ )$$

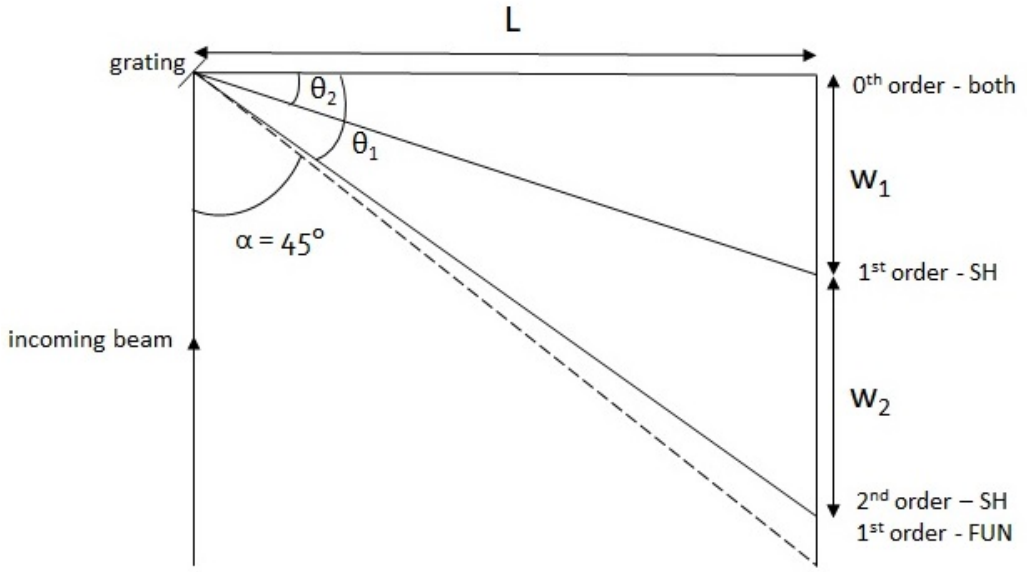

Figure 5.1.: Sketch of diffraction grating

with $d = 1/600$ mm/lines and $\alpha = 45°$. Then,

$$\lambda_{FUN} = \frac{1/600}{1}(sin\ 45° - sin\ (45 - \theta_1)°)$$

$$\Delta\lambda_{FUN} = \frac{1}{600} cos\ (45 - \theta_1)\Delta\theta_1$$

$$\lambda_{SH}^{(1)} = \frac{1/600}{1}(sin\ 45° - sin\ (45 - \theta_2)°)$$

$$\lambda_{SH}^{(2)} = \frac{1/600}{2}(sin\ 45° - sin\ (45 - \theta_1)°)$$

$$\Delta\lambda_{SH}^{(1)} = \frac{1}{2 \cdot 600} cos\ (45 - \theta_1)\Delta\theta_1$$

$$\Delta\lambda_{SH}^{(2)} = \frac{1}{600} cos\ (45 - \theta_2)\Delta\theta_2$$

$$\lambda_{SH} = \frac{\lambda_{SH}^{(1)} + \lambda_{SH}^{(2)}}{2}$$

The theoretical resolution of the grating is $A = n\dot{N}$ where n is the order of the spot and N is the number of lines illuminated by the grating. Since we used lenses of the same focal length, $N = (3.5 \pm 0.5)\ mm \times 600\ lines/mm = (2100 \pm 300)$ lines. The experimental resolution is $A = \lambda/\Delta\lambda$. The values of the wavelengths and respective resolutions are given in table 5.1.
The ratio of wavelengths is:

$$\frac{\lambda_{FUN}}{\lambda_{SH}} = 2.051 \pm 0.035$$

The fundamental wave wavelength is essentially double that of the harmonic wave. Thus, frequency doubling has been achieved well.

$Order, n$	Wavelength, λ (nm)	$A_{th} = n \cdot N$	$A_{exp} = \frac{\lambda}{\Delta\lambda}$
FUN 1st	921.868 ± 11.34	2100 ± 300	81.29
SH 1st	438.182 ± 8.73	2100 ± 300	50.19
SH 2nd	460.934 ± 5.67	4200 ± 600	81.29
SH mean	449.558 ± 5.20		88.45

Table 5.1.: Wavelength and resolution of different beams

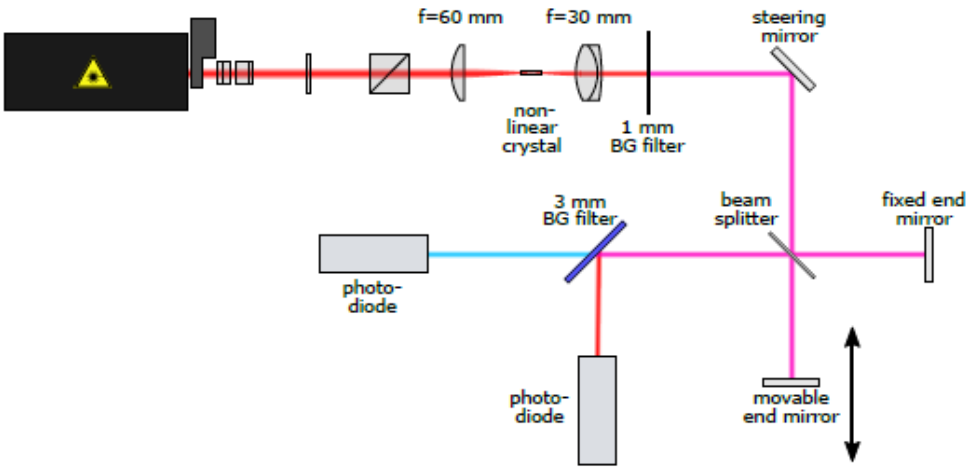

Figure 5.2.: Setup of Michelson Interferometer [1]

5.2. Interferometric Comparison using Michelson Interferometer

Diffraction grating is a rather crude method of comparing wavelengths. To get more precise measurements, Michelson interferometer was set up as shown in fig. 5.2. The beam coming from the laser is collimated using a 30mm lens. The beam splitter is aligned so that the beams from the two end mirrors overlap perfectly at the output of the interferometer. The 3mm BG filter is used to split the fundamental and harmonic beams and they are read by the two photo-diodes. The interference signals are read off the oscilloscope by moving the movable end mirror.

By switching to the X-Y mode on the oscilloscope, Lissajous figures such as fig. 5.3 were observed. The movable end mirror was moved slowly and every time the same figure appeared, i.e., when we cross one order or $\pi/2$ phase difference, the position of the mirror was noted. The readings are given in table A.5.

The data was fitted with a linear function of the form:

$$f(x) = a \cot n + c$$

with n being the order of the figure. The plot is shown in fig. 5.4. The fit parameters were obtained to be:

$$a = (-1.25 \pm 0.014)\ cm$$

$$c = (38.95 \pm 0.15)\ cm$$

Figure 5.3.: Lissajous figure as seen on the oscilloscope

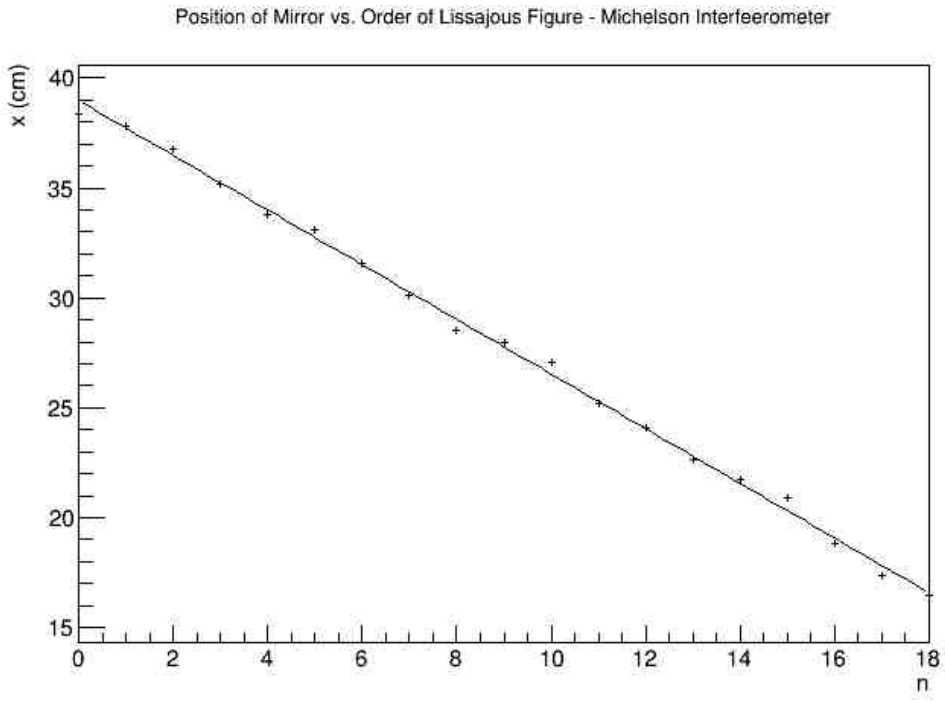

Figure 5.4.: Position of movable end mirror vs. order (every time the same shape of Lissajous figure appeared)

The phase difference between every order was $\frac{\pi}{2}$. So,

$$\frac{\pi}{2} = \phi_{SH} - 2\phi_{FUN} = 2a(k_{SH} - k_{FUN})$$

ϕ is the phase and k is the wave vector of the two waves.

$$\implies \frac{\pi}{2} = 2a \cdot 2\pi \left(\frac{2n_{SH}}{2\lambda_{SH}} - \frac{2n_{FUN}}{\lambda_{FUN}}\right) = 8\pi a\left(\frac{n_{SH} - n_{FUN}}{\lambda_{FUN}}\right)$$

$$\therefore \Delta n_{exp} = n_{SH} - n_{FUN} = \frac{\lambda_{FUN}}{16a} = (4.964 \pm 0.000009) \times 10^{-6}$$

The individual refractive indices are:

$$1 - n_{FUN} = \frac{\lambda_{vac,FUN}}{8a} = (9.87 \pm 0.000018) \times 10^{-6}$$

$$1 - n_{SH} = \frac{\lambda_{vac,SH}}{8a} = (4.935 \pm 0.000009) \times 10^{-6}$$

Using the formula given in the script for calculating refractive index of air:

$$10^8(n(\lambda_{vac}) - 1) = 8342.13 + \frac{2406030}{130 - s^2} + \frac{15997}{38.9 - s^2} \;\; ; \;\; s = \frac{1}{\lambda_{vac}[\mu m]}$$

This gives the theoretical values of the refractive indices as:

$$n_{vac,SH} - 1 = 2.79 \times 10^{-4}$$

$$n_{vac,FUN} - 1 = 2.74 \times 10^{-4}$$

$$\Delta n_{th} = n_{vac,SH} - n_{vac,FUN} = 4.94 \times 10^{-6}$$

The experimental and theoretical values are not within the same error interval but the difference is not too significant. The deviation in the experimental and theoretical values could be because of the crude way in which the measurements were made. The interferometer is sensitive to movements and external light. There were also some difficulty in obtaining the exact Lissajous figure every time. The ratio of wavelengths is:

$$\frac{\lambda_{FUN}}{\lambda_{SH}} = \frac{n_{SH}}{n_{FUN}} = \frac{\Delta n}{n_{FUN}} + 1$$

For Δn_{exp}, the ratio is (2.0059 ± 0.011). It is in agreement with the expected value.
The spectroscopic resolution $A = \frac{\lambda_{SH}}{\Delta\lambda}$.

$$\begin{aligned} \Delta\lambda &= \lambda_{FUN} - 2\lambda SH \\ &= \frac{\lambda_{vac,FUN}}{n_{FUN}} - 2\frac{\lambda_{vac,SH}}{n_{SH}} \\ &= \lambda_{vac,FUN}\left(\frac{1}{n_{FUN}} - \frac{1}{n_{SH}}\right) \\ &= \lambda_{vac,FUN}\frac{\Delta n}{n_{FUN}n_{SH}} \end{aligned} \tag{5.1}$$

Therefore,

$$\Delta\lambda_{exp} = (4.90 \pm 0.4) \times 10^{-12}$$

$$\Delta\lambda_{th} = 4.87 \times 10^{-12}$$

and hence,

$$A_{exp} = (100.71 \pm 1.97) \times 10^3$$

$$A_{th} = 101.334 \times 10^3$$

The deviation from the 1:2 ratio is seen to be significantly less and good frequency doubling has been achieved.

6. Conclusion

We first measured and optimized the diode laser ans the variable attenuator by measuring the power of the laser and calibrating the attenuator. Then we doubled the frequency of the laser light wavelength 987 nm in the infrared region to wavelength 483.5 nm in the visible blue region using a $KbNO_3$ crystal. The properties of the second harmonic was studied; the power of the harmonic was measured with respect to the temperature of the crystal, and the power and polarization of the fundamental. The wavelength of the harmonic beam was then measured using a diffraction grating. A more precise interferometric comparison was made using Michelson interferometer. We found that the ratio of the wavelengths of the fundamental to harmonic was close to 1:2, there was no significant deviation. We conclude that fairly good frequency doubling was achieved.

A. Appendix

I_{inj} /mA	P /μW	ΔP /μW
0	0	0.001
10	0.003	0.001
20	0.0078	0.001
30	0.0135	0.001
40	0.0212	0.001
50	0.0317	0.001
60	1.5	0.01
70	8.5	0.01
80	15.4	0.1
90	21.6	0.1
100	29	0.1
110	34.4	0.1
120	41.6	0.1
130	47.5	0.1
140	54.2	0.1
150	61.3	0.1
160	66.3	0.1
170	75.3	0.1
190	88.8	0.1
210	99.	0.1
220	106	1
230	115	1
240	120	1
250	132	1
260	134	1
270	140	1
280	145	1

Table A.1.: Laser output power vs. injection current

θ /°	P_{FUN} /μW	P_{SH} /μW
0	38.3	2.4
2.5	45.8	3.6
5	53.1	4.84
7.5	60.8	6.17
10	70.1	7.51
12.5	77.5	8.77
15	82.1	10.4
17.5	85.2	12
20	89	12.7
22.5	91	13.4
25	92	13.7
27.5	91	13.6
30	90	12.9
32.5	86	12.3
35	83.2	11
37.5	77.9	9.5
40	69.3	8.33
42.5	62.7	6.4
45	54.7	5.22
47.5	46.9	3.84
50	40.2	2.64
52.5	33.1	2.01
55	25	1.13
57.5	18.3	0.79
60	10.8	0.48
62.5	6.8	0.32
65	3.36	0.27
67.5	1.56	0.26
70	0.74	0.25
72.5	1.24	0.2
75	3.23	0.26
77.5	6.4	0.3
80	10.6	0.42
82.5	16.8	0.62
85	22.5	0.98
87.5	27.9	1.5
90	38.4	2.4
92.5	46.2	3.48
95	52.2	4.69
97.5	60.5	6.32
100	68.5	7.85
102.5	75.7	9.1
105	81.1	10.4

107.5	86.6	11.8
110	89.6	12.7
112.5	92.5	13.4
115	92.9	13.8
117.5	92	13.5
120	90.2	12.8
122.5	85.6	12.1
125	81	11
127.5	77.2	9.6
130	70	8.2
132.5	63.2	6.6
135	54.6	5.2
137.5	46.7	3.9
140	38.3	2.7
142.5	29.3	1.83
145	23.3	1.17
147.5	16.6	0.66
150	12.7	0.46
152.5	5.4	0.32
155	2.7	0.2
157.5	1.04	0.24
160	0.27	0.23
162.5	0.84	0.24
165	2.47	0.24
167.5	6.57	0.29
170	10.9	0.42
172.5	16.2	0.6
175	22.8	1.01
177.5	29.7	1.47
180	36.2	2.36
182.5	44.6	3.49
185	51.4	4.62
187.5	60.2	5.96
190	69.2	7.57
192.5	75.2	9.29
195	81.5	10.6
197.5	86.5	11.9
200	89.4	12.8
202.5	91.7	13.4
205	92.6	13.7
207.5	92.6	13.6
210	90.6	13.1
212.5	86.7	12.2
215	83.4	10.9
217.5	78	9.9

220	70.6	8
222.5	62.5	6.5
225	54.9	5.2
227.5	48	3.7
230	39.8	2.6
232.5	31.9	1.8
235	24.5	1.1
237.5	17.7	0.8
240	12.3	0.49
242.5	6.6	0.44
245	3.7	0.27
247.5	1.41	0.2
250	0.78	0.35
252.5	1.17	0.25
255	2.54	0.26
257.5	5.13	0.3
260	8.99	0.42
262.5	17.3	0.66
265	22.6	0.97
267.5	28.6	1.53
270	37	2.24
272.5	46.8	3.48
275	54.4	5.05
277.5	61.6	5.48
280	70.4	6.91
282.5	76.2	8.8
285	82.8	10.1
287.5	88.8	10.5
290	91.2	12
292.5	93.4	12.7
295	93.7	13.1
297.5	92.8	12.6
300	90.3	12.1
302.5	87	11.2
305	83.7	9.7
307.5	76.7	8.7
310	70.3	6.89
312.5	61.4	5.86
315	51.5	4.52
317.5	49	3.31
320	38.2	2.25
322.5	29.4	1.57
325	20.6	1.08
327.5	17.5	0.65
330	10.8	0.41

332.5	6.27	0.29
335	3.57	0.25
337.5	1.28	0.22
340	0.28	0.21
342.5	0.72	0.24
345	2.67	0.26
347.5	6.02	0.29
350	10.9	0.37
352.5	17.8	0.6
355	23.6	0.97
357.5	31.4	1.63
360	36.9	2.18

Table A.2.: Power of fundamental and harmonic beams vs. angle of polarization

$T\ /°C$	$P_{SH}\ /\mu W$
27	0.27
27.2	0.27
27.4	0.27
27.6	0.27
27.8	0.27
28	0.27
28.2	0.27
28.4	0.27
28.6	0.27
28.8	0.27
29	0.27
29.2	0.27
29.4	0.28
29.6	0.28
29.8	0.28
30	0.28
30.2	0.28
30.4	0.28
30.6	0.28
30.8	0.28
31	0.28
31.2	0.28
31.4	0.27
31.6	0.27
31.8	0.29
32	0.3
32.2	0.3
32.4	0.29
32.6	0.28

32.8	0.28
33	0.28
33.2	0.3
33.4	0.31
33.6	0.3
33.8	0.3
34	0.31
34.2	0.38
34.4	0.45
34.6	0.51
34.8	0.52
35	0.56
35.2	0.86
35.4	1.74
35.6	3.12
35.8	5.3
36	9
36.2	11.1
36.4	13.2
36.6	13.5
36.8	12.5
37	10
37.2	5.6
37.4	3.8
37.6	1.88
37.8	0.86
38	0.43
38.2	0.51
38.4	0.59
38.6	0.61
38.8	0.53
39	0.39
39.2	0.29
39.4	0.3
39.6	0.34
39.8	0.37
40	0.33

Table A.3.: Harmonic power vs. crystal temperature

θ /°C	P_{SH} /μW
0	2.6
2.5	3.5
5	4.8
7.5	6
10	7.5
12.5	8.6
15	10
17.5	10.9
20	11.6
22.5	12
25	12
27.5	11.6
30	10.9
32.5	10
35	8.8
37.5	7.5
40	6.5
42.5	5.2
45	4.1
47.5	3
50	1.8
52.5	1.2
55	0.8
57.5	0.6
60	0.4
62.5	0.28
65	0.26
67.5	0.23
70	0.23
72.5	0.22
75	0.24
77.5	0.3
80	0.48
82.5	0.75
85	1.1
87.5	1.71
90	2.6
92.5	3.64
95	4.75
97.5	5.9
100	7.54
102.5	8.96
105	9.84

107.5	10.8
110	11.4
112.5	11.8
115	11.8
117.5	11.6
120	10.8
122.5	10
125	8.59
127.5	7.61
130	6.26
132.5	4.73
135	3.84
137.5	2.76
140	1.68
142.5	1.18
145	0.76
147.5	0.47
150	0.35
152.5	0.25
155	0.23
157.5	0.23
160	0.22
162.5	0.23
165	0.24
167.5	0.3
170	0.48
172.5	0.75
175	1.19
177.5	1.75
180	2.63
182.5	3.48
185	4.8
187.5	5.99
190	7.02
192.5	8.7
195	9.81
197.5	10.7
200	11.3
202.5	11.7
205	11.8
207.5	11.5
210	10.9
212.5	10
215	8.75
217.5	7.07

220	6.21
222.5	5.02
225	3.86
227.5	2.93
230	1.98
232.5	1.04
235	0.81
237.5	0.52
240	0.34
242.5	0.29
245	0.27
247.5	0.26
250	0.26
252.5	0.26
255	0.29
257.5	0.37
260	0.52
262.5	0.83
265	1.14
267.5	1.97
270	2.76
272.5	3.99
275	5.03
277.5	6.41
280	7.56
282.5	8.93
285	9.9
287.5	11
290	11.6
292.5	12
295	12
297.5	11.7
300	11
302.5	10.1
305	9.2
307.5	7.46
310	6.07
312.5	4.71
315	3.7
317.5	2.64
320	1.84
322.5	1.19
325	0.8
327.5	0.44
330	0.35

332.5	0.27
335	0.26
337.5	0.25
340	0.26
342.5	0.25
345	0.23
347.5	0.33
350	0.52
352.5	0.89
355	1.29
357.5	1.71
360	2.81

Table A.4.: Power of harmonic wave vs. polarization of fundamental wave (angle of half-wave plate)

n	$x\ /cm$
0	38.4
1	37.8
2	36.8
3	35.2
4	33.8
5	33.1
6	31.6
7	30.1
8	28.5
9	28
10	27.1
11	25.22
12	24.1
13	22.6
14	21.7
15	20.9
16	18.8
17	17.4
18	16.5

Table A.5.: Position of movable end mirror vs. order of interference - Michelson interferometer

Bibliography

[1] University of Bonn: *A245 - Optical Frequency Doubling – Experiment Description*, 2015

[2] R. W. Boyd: *Nonlinear Optics* 2nd ed., Academic Press, 2003

[3] A. Yariv: *Optical Electronics* 4th ed., Saunders College Publishing, 1991

[4] D. Meschede: *Optics, Light and Lasers*, Wiley VCH, 2007

[5] S. Hooker and C. Webb: *Laser Physics*, Oxford Master Series, 2010

[6] A. Yariv: *Quantum Electronics* 3th ed., John Wiley & Sons, 1989